Available online at www.sciencedirect.com
SCIENCE DIRECT®
Thermochimica Acta 401 (2003) 149–158
thermochimica acta
www.elsevier.com/locate/tca

Square modulated differential thermal analysis

J. del Cerro*, J.M. Martín-Olalla, F.J. Romero

Departamento de Física de la Materia Condensada, Instituto Mixto de Ciencia de Materiales, CSIC-Universidad de Sevilla, P.O. Box 1065, Sevilla 41080, Spain

Received 26 June 2002; accepted 12 November 2002

Abstract

$KMnF_3$ and DKDP crystals have been studied around their phase transitions using a conduction calorimetry technique where a long periodical square thermal pulse (0.05 K in amplitude) is superposed to a heating or cooling ramp as low as $0.06\,K\,h^{-1}$. Specific heat data obtained in the dissipation and relaxation semiperiods of the square pulse become different inside the phase transition interval. The electromotive force developed by the heat fluxmeters at the end of the relaxation semiperiod (underlying signal) is compared with the DTA trace obtained in a second run with the same temperature ramp but without the modulated perturbation. The comparison between the DTA trace and specific heat data obtained in the first run allows us to determine the value of the latent heat and to obtain information about the kinetic of the phase transition.

Keywords: Latent heat; Specific heat; Conduction calorimetry; MDSC; DTA

1. Introduction

DTA and DSC devices measure the change of enthalpy ΔH of a sample when its temperature is modified. If a first-order phase transition takes place, this change of enthalpy has two contributions: one due to the variation with the temperature of the heat capacity c and other due to the latent heat L.

Defects, temperature gradients, internal stresses, etc make the transition take place over a temperature range (T_1, T_2). When the first contribution to ΔH is small enough, this temperature range can be determined in the DTA trace and L can be evaluated. In other cases, the starting and ending points of the latent heat effect merge with the increase of c near the transition and it is difficult to determine that temperature interval. This is the case of a transition near a tricritical point, where c presents a strong anomaly around the transition point T_0 and the latent heat is very small. To evaluate the temperature range (T_1, T_2) where the latent heat is present it is necessary to compare the DTA or DSC trace with specific heat data obtained under similar thermal conditions.

Modulated differential scanning calorimetry (MDSC) [1–3] tries to solve this problem; this technique is a conventional DSC where the temperature ramp is modulated by an alternative component (ACC):

$$T(t) = T_0 + bt + B\sin\omega t$$

under the condition $b > B\omega$ to avoid an inversion in the temperature variation of the sample.

By means of a direct Fourier transform algorithm the continuous component (DSC) and the alternative component (ACC) are analysed separately. As a kinetic process affects in a different way to DSC and ACC components, the comparison of both components allows to discriminate the temperature range where

* Corresponding author.
E-mail address: delcerro@us.es (J. del Cerro).

0040-6031/03/$ – see front matter © 2002 Elsevier Science B.V. All rights reserved.
PII: S0040-6031(02)00545-2

the kinetic process, such a phase transformation, is present. The comparison of the underlying MDSC heat flux with conventional heat flux DSC and AC calorimetry shows a satisfactory agreement in both cases although with a lower resolution than in high precision AC calorimetry [2].

During the last two decades we have developed a calorimetric technique which uses heat fluxmeters and where a low temperature ramp is modulated by a periodical serial of square thermal pulses [4,5]. The sample passes from a uniform temperature distribution to another one and the integration of the electromotive force (emf), given by the fluxmeters between both temperature distributions, allows to determine absolute values of the specific heat c of the sample. We must point out that we obtain two c data in each cycle: one from the dissipation branch (c_d) and another from the relaxation branch (c_r) of the cycle.

Due to the thermal ramp, the emf V_0 measured before every dissipation semiperiod can be considered as the underlying DTA heat flux and, consequently, we can call this procedure square modulated differential thermal analysis.

The high number of thermocouples (a hundred) forming the fluxmeters allows the device to work at a very small temperature variation rate (about $0.1\,K\,h^{-1}$). We can carry out a second run with the same temperature ramp but without modulation in such a way that the equipment works as a very sensitive DTA device.

The comparison between the DTA trace V_D obtained in the second run and specific heat data obtained in the first one allows us to determine the temperature interval where the latent heat or whatever kinetic process is present and to evaluate accurately the latent heat, even when the specific heat present a strong anomaly. This study has been successfully carried out previously [6,7].

In this paper, we apply this technique in the case of two samples whose phase transitions present a very different behaviour: ferroelectric DKDP and ferroelastic $KMnF_3$ crystals.

We will compare the underlying signal V_0 with the DTA trace V_D in both cases and we will analyse the behaviours of the specific heat data c_d and c_r during the phase transitions.

2. Experimental arrangement

The experimental arrangement (Fig. 1) has been described in detail [8]. The sample is pressed between two identical heat fluxmeters, which are made from 50 chromel–constantan thermocouples [9] connected in series with the wires placed in parallel lines. One of the fluxmeters is fixed to a calorimeter block while the other is pressed by a bellow, which allows to apply uniaxial stress to the sample. The fluxmeters, which have a cross-section of $1\,cm^2$, are rigid enough to apply a controlled uniaxial stress on the sample in the range between 0 and 12 bar. Two electrical resistances (heaters) are placed between each face of the sample and fluxmeters. These resistances can dissipate a uniform heat power on the sample face. The entire assembly is placed in a cylindrical hole made in a cylindrical piece of bronze (10 kg) which serves as the heat sink (the calorimeter block). Its temperature is measured with a commercial platinum thermometer (Leeds

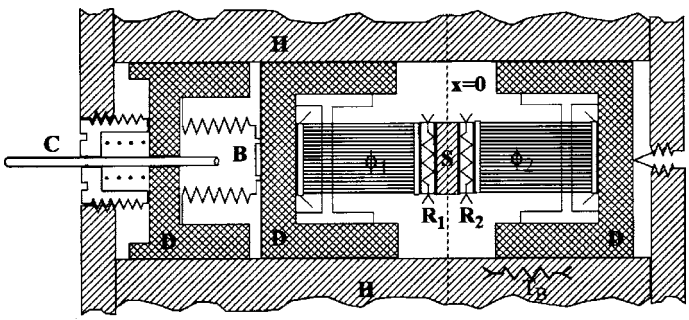

Fig. 1. Diagram of the sensor: Φ_1 and Φ_2, heat fluxmeters; R_1 and R_2, heaters; S, sample; B, bellow; D, fluxmeter and bellow container; H, heat sink; C, capillary.

and Northhurp model 8164B) and a Tinsley resistance bridge (model Ambassador). The block and two surrounding radiation shields are placed into a hermetic outer case under vacuum (10^{-7} torr). A HPE-1328A current source and HPE-1326 multimeter are used, respectively, to produce and to measure the power dissipated in the heaters. The electromotive force (emf) produced by the fluxmeters is measured by a Keithley 2182 nanovoltmeter. All the devices are controlled by a HP-75000 data acquisition system.

The high vacuum inside the block, the high numbers of thermocouples and the symmetrical distribution of fluxmeters and sample assure the unidimensional heat conduction through the fluxmeters. The high thermal capacity of the block assures the thermal stability in the sample. The measurements are carried out on quasistatic conditions changing the temperature of the block at a very low constant rate ($\partial T/\partial t < 0.1\,\mathrm{K\,h^{-1}}$).

3. Measurement method

3.1. Isothermal measurement

Let us consider a simple case in which the temperature distribution along the calorimeter is kept constant. The heat flux flowing through the fluxmeter will be zero. Thus, the electromotive force given by the fluxmeter will be ideally $V_0 = 0$. The specific heat is measured by exciting the sample with an external dissipation of heat in the heaters. The dissipation is a square pulse of amplitude W_0 and period 2τ.

After $t = 0$, the temperature distribution along the calorimeter and the heat flux will change in time within a transient regime until a new steady-state distribution of temperature is reached. The typical time to reach the steady-state is a characteristic time, which is related to the thermal diffusivity of fluxmeters and sample [4]. At the steady-state, the power W_0 dissipated by the heaters will flow through the fluxmeter, which will give a proportional electromotive force V_1. The Fourier law of heat flow also relates W_0 (and hence V_1) with the temperature difference at the edges of the fluxmeters through the thermal conductivity of the fluxmeters. Let us call this temperature difference ΔT.

In Fig. 2 we represent as a function of time an ideal square pulse (a) and the response of the fluxmeters (b) (which represent the change of temperature of the sample and the heat flowing through the fluxmeters).

We measure the specific heat by integrating the transient response. Two different quantities can be considered: the area, A_d, obtained while the heaters are

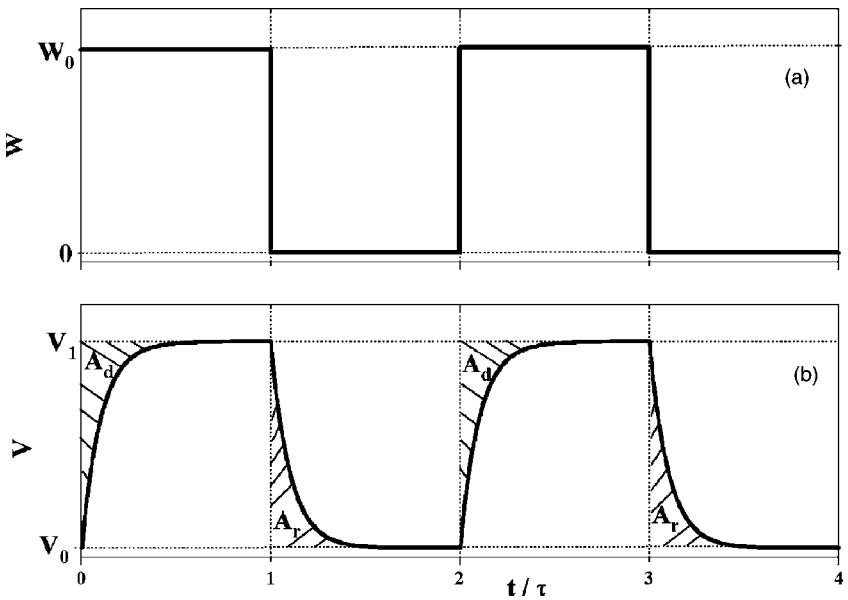

Fig. 2. An ideal square pulse and the experimental response of the fluxmeters which represents the change of temperature of the sample and the heat flux through the fluxmeters.

dissipating (dissipation branch) and the area, A_r, obtained while there is no dissipation (relaxation branch). In an ideal experiment both areas must match. The specific heat of the sample is obtained by comparing this experience with a calibrating experience in which no sample is put into the calorimeter. The specific heat of the sample is given by

$$c_r = \frac{2}{\beta}(A_r - A_r^0), \qquad c_d = \frac{2}{\beta}(A_d - A_d^0) \tag{1}$$

where β is the thermal resistance of the fluxmeter (obtained by calibration) [8] and

$$A_r = \int_{\tau}^{2\tau} \frac{V(t)}{V_1}\,dt, \qquad A_d = \tau - \int_0^{\tau} \frac{V(t)}{V_1}\,dt \tag{2}$$

and A_r^0, A_d^0 are those integrals when no sample is put into the calorimeter (calibration). Correspondingly, we obtain two values of the specific heat, that on the dissipating branch, c_d, and on the relaxation branch, c_r. In normal conditions both data match but we will show that they disagree during a first-order phase transition.

3.2. Drifting the temperature of the calorimeter

Let us consider now that the temperature of the calorimeter is changing continuously in time within a smooth function with $dT/dt = \text{cte}$ due to an external imposed condition (for instance, the calorimeter is sunk in an alcohol bath whose temperature is lowering by inputting liquid nitrogen). In the simplest case, the temperature gradient along the calorimeter is constant and a quantity of heat (necessary for changing the temperature of the sample) will be flowing through the fluxmeter giving a non-zero electromotive force V_0. Under this circumstance the specific heat of the sample is measured by superposing the square pulse of amplitude W_0 and period 2τ. We only have to subtract the offset value V_0 to get the appropriate value of the areas A_d and A_r.The offset value V_0, which as we will see below can be considered as the DTA underlying component, is a smooth function of time so that an appropriate determination of its value at $t = 2n\tau$ ($n = 0, 1, 2, \ldots$) should be sufficient to get its evolution on time. The determination of the steady-state electromotive force V_1 at $t = (2n+1)\tau$ where ($n = 0, 1, 2, \ldots$) is sufficient to get its evolution on time as well.

3.3. Working values of the parameters

Let us analyse now the order of magnitude of the parameters involved in the determination of the specific heat of the sample. The most important of them is the characteristic time of the calorimeter. It is related to the thermal diffusivity of the fluxmeter, which has the highest thermal capacity under normal conditions. Experimentally we got this time as 1 min approximately. Thus, a periodic pulse of semiperiod similar to 10 min is sufficient to get the steady-state temperature distribution under normal conditions.

We usually perform experiments in which the temperature of the calorimeter is continuously increasing or decreasing at a rate of about $0.1\,\mathrm{K\,h^{-1}}$. The temperature difference between the middle of the sample and its borders due to the temperature ramp is estimated to be lower than $5 \times 10^{-4}\,\mathrm{K}$, so that we consider that the temperature in the sample is practically uniform. Under such conditions the measurement of the specific heat should be considered 'static' as opposed to 'dynamic' measurement of specific heat made by ac calorimetry.

On the other hand, taking into account the semiperiod of the pulse signal $\tau = 10\,\mathrm{min}$ and that we use a value dT/dt of about $0.05\,\mathrm{K\,h^{-1}}$, the change of temperature during the measurement $\Delta T_\tau = \tau(d\mathrm{T}/d\mathrm{t})$ is around 0.01 K.

The increase of temperature ΔT due to the heat dissipated on the heaters during the dissipation branch is evaluated to be about 0.05 K.

According to this, during the relaxation branch when cooling and dissipation branch when heating ΔT and ΔT_τ have the same sign (positive superposition). During relaxation branch when heating and dissipation branch when cooling ΔT and ΔT_τ have opposite sign (opposite superposition) and the temperature variation of the sample is reversed because $\Delta T > \Delta T_\tau$.

3.4. DTA measurement

Due to the high number of thermocouples forming the fluxmeters and the high thermal stability of the assembly, at a second run, the emf V_D (DTA trace) can be measured continuously without dissipation in the heaters and using the same temperature ramp (about $0.1\,\mathrm{K\,h^{-1}}$) as we measure the specific heat. The equipment

works like a very sensitive DTA device. The DTA trace and specific heat data are comparable since both sets of data are obtained with the same device, on the same sample and under similar thermal conditions.

From the specific heat data obtained in the first run, we calculate the emf V_c, which would correspond to the DTA trace due exclusively to the thermal capacity behaviour [6]. Comparing the measured V_D and the calculated V_c, we deduce that only in the temperature range (T_1, T_2) where they do not coincide there is effect from the latent heat. The latent heat is determined by integrating the emf V_D between T_1 and T_2 and using the straight line $V_D(T_1) - V_D(T_2)$ as baseline.

3.5. Characteristics of the samples

The crystal $KMnF_3$ undergoes a ferroelastic phase transition from the cubic perovskite structure to a tetragonal structure at 186 K [10]. The order parameter is related to the angle ϕ of the MnF_6 octahedral rotation around the <0 0 1> axis [11]. The transition is first-order but it has been shown that it is near a tricritical point [12–14]. The order of the transition can be changed by substituting Mn for Ca [6,15–18].

The studied sample of $KMnF_3$ was a single crystal, 5 mm thick, with a cross section of 0.8 cm^2 and a mass $m = 1.47$ g. Using the previously described method, we evaluated the latent heat as $L = 0.129 \pm 0.002$ J g^{-1} [6].

The ferroelastic crystal potassium dihydrogen phosphate (KDP) shows a well-established first-order phase transition at 123 K from a tetragonal paraelectric phase at high temperature to an orthorhombic ferroelastic phase at low temperatures [19]. When KDP is deuterated (DKDP), both the latent heat and transition temperature increase with the degree of deuteration [20].

The studied sample of DKDP was a single crystal, 3 mm thick, with a cross-section of 0.8 cm^2 and a mass of $m = 0.66$ g. Its degree of deuteration is estimated to be 82%. The value of the latent heat was evaluated in a previous work as $L = 2.3$ J g^{-1} [21].

4. Results

4.1. $KMnF_3$

In Fig. 3 we represent the temperature evolution of specific heat obtained in the dissipation branch (c_d) and in the relaxation branch (c_r) when heating (a) and cooling (b) at a constant rate of $dT/dt = 0.06$ K h^{-1}. Specific heat data in a larger temperature interval have been shown previously [6].

In Fig. 4, we represent the measured DTA traces V_D versus temperature of the sample when heating (a) and cooling (b) the $KMnF_3$ sample at the same constant rate of 0.06 K h^{-1} without dissipation in any heater. In

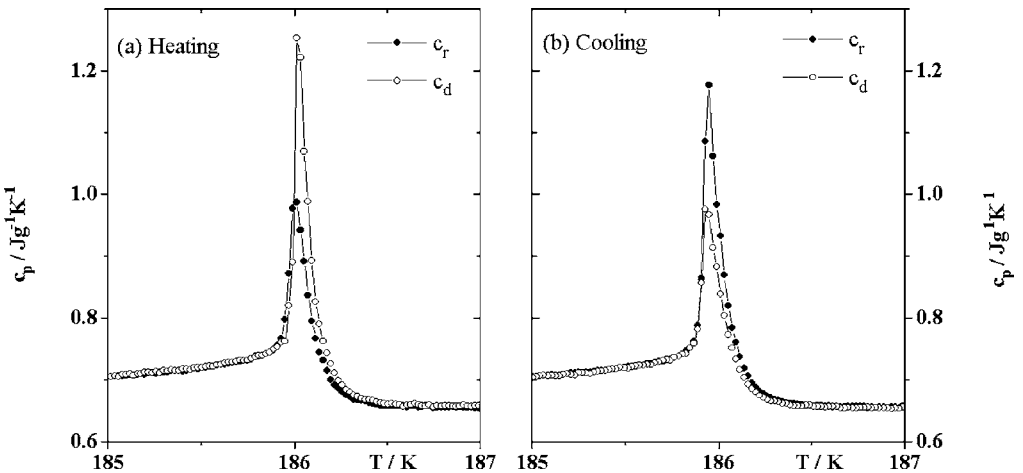

Fig. 3. Specific heat obtained in the relaxation branch (c_r, filled circles) and in the dissipation branch (c_d, open circles) for $KMnF_3$: (a) heating, (b) cooling. The lines are guides for the eyes.

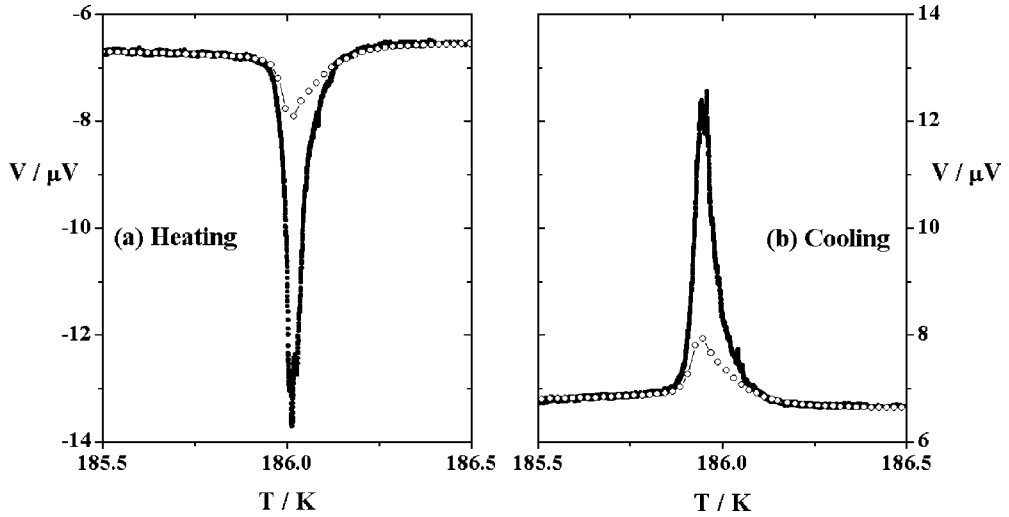

Fig. 4. Measured DTA trace V_D (filled circles) and calculated V_c (open circles) vs. temperature of the block for $KMnF_3$: (a) heating and (b) cooling.

this figure, we also represent the traces V_c calculated from the specific heat data in Fig. 3. According to above (Section 3.3), in the temperature range where V_D and V_c are different, there is effect from the latent heat. We must point out that these temperature ranges agree with those heating and cooling ones where c_d and c_r become different (Fig. 3).

The agreement between c_d and c_r outside the phase transition interval show that positive and opposite superposition of temperature ramp and modulation do not affect the specific heat measurements and data will be similar to those obtained under isothermal conditions.

We must point out that data obtained with positive superposition (c_r cooling and c_d heating) match very well and data obtained under opposite superposition (c_r heating and c_d cooling) match as well even during the phase transition. Data obtained under opposite superposition are lower than those obtained under positive superposition. This difference will be discussed below.

4.2. DKDP

In Fig. 5 we represent c_d and c_r versus temperature obtained when heating (a) and cooling (b) DKDP sample at a constant rate of $dT/dt = 0.06\,K\,h^{-1}$. Specific heat data in a larger temperature interval have been shown previously [21].

In Fig. 6, we represent the DTA trace V_D and the underlying signal V_0 versus temperature for heating and cooling at a constant rate of $0.06\,K\,h^{-1}$. These data are represented respect to the baseline obtained from the comparison of V_D with the calculated V_c.

Outside the phase transition interval, c_d and c_r data agree in both heating and cooling runs as $KMnF_3$ data do. However, in that temperature interval, c_d and c_r show a non-regular behaviour.

We must keep in mind that defects in the sample as slight inhomogeneities in the degree of deuteration may make the evolution of the transition non-uniform. This fact produces the appearance of several peaks in the behaviour of V_D as we can see in Fig. 6.

During the measurement of the specific heat we can expect a similar effect on the baseline respect to which the integrals A_r and A_d (expressions 1 and 2) are calculated to evaluate the specific heat. Although these calculations are not affected by linear variations of the baseline, the behaviour of V_D in DKDP sample (it presents peaks as big as 15 μV) clearly suggests a strong non-linear behaviour of the baseline and, thus, c_d and c_r data of DKDP sample during the phase transition are affected by the high value of the latent heat and by an uncontrolled error, so that we consider that

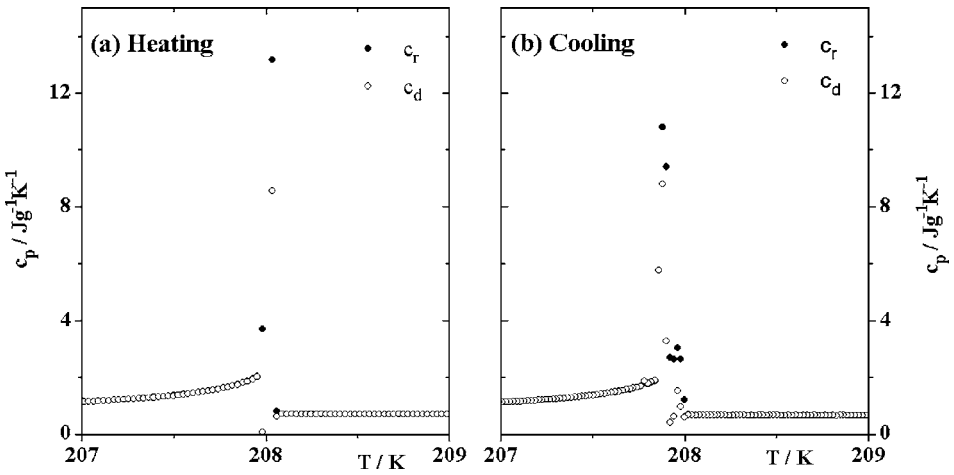

Fig. 5. Specific heat obtained in the relaxation branch (c_r, filled circles) and in the dissipation branch (c_d, open circles) for DKDP: (a) heating and (b) cooling.

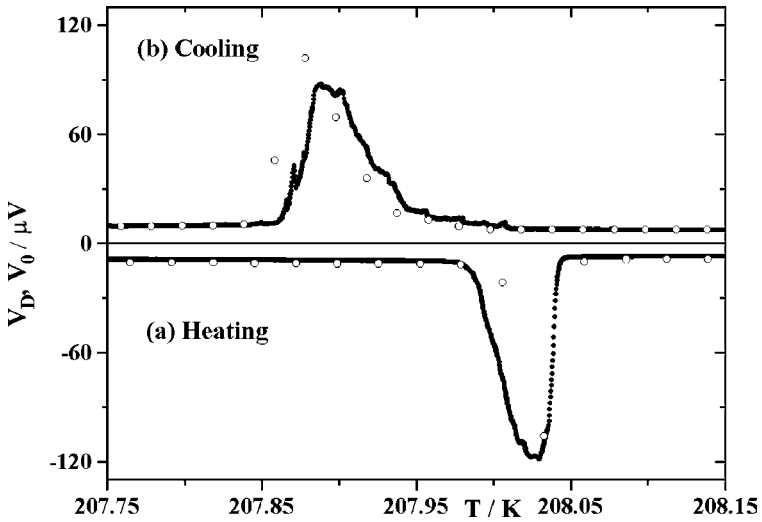

Fig. 6. Measured DTA trace V_D (filled circles) and underlying signal V_0 vs. temperature of the block for DKDP: (a) heating and (b) cooling.

a full explanation of c_d, c_r data during the phase transition cannot be done.

In the case of $KMnF_3$ sample, the latent heat is much smaller than in DKDP and the maximum value of the DTA trace is 7 μV and although there are several peaks they are lower than 1 μV. This suggests a almost linear behaviour of the baseline in each cycle, so that we obtain a regular behaviour of c_d and c_r in $KMnF_3$ sample.

5. Square modulated thermal analysis

The measurement sequence of specific heat described above can be considered as a MDSC technique where the sinusoidal perturbation is changed by a regular long-period series of squared waved pulses. According to this, the electromotive force V_0 at the end of each pulse (see Fig. 2) can be considered as the underlying value of the DTA component.

The long period of the sequence (approximately 20 min) makes no relevant any effect from the thermal conductivity and it allows to measure accurately absolute values of the specific heat, but it does not allow to collect a sufficient number of experimental data V_0 to evaluate the latent heat directly from the first run. However, it is interesting to compare V_0 and V_D data, which are obtained at the same temperature variation rate, to study the influence of the temperature inversion on the underlying signal and to deduce when V_0 gives us a correct information about the latent heat.

In Fig. 6, we also represent the underlying signal V_0 versus temperature when heating (a) and cooling (b) the DKDP sample. In spite of the small number of points, data when cooling suggest a similar behaviour of V_D and V_0. Despite the temperature variation is reversed in each pulse, the modulated perturbation seems to have relatively small influence on the underlying signal, although it produces a shift of 0.02 K in the transition temperature. When heating the comparison is not possible since we only have three V_0 data in the phase transition interval.

Let us now analyse in more detail $KMnF_3$ data. In Fig. 7, the underlying signal V_0 and the corresponding DTA trace are represented versus temperature for heating and cooling. On cooling the behaviour of V_0 (end of positive superposition) is very similar to the DTA trace but on heating the V_0 anomaly does not appear.

On the other hand, the electromotive force V_1 at the end of the dissipation branch (see Fig. 2) is also represented in Fig. 7. As $V_1 - V_0 = \alpha W_0$, where α is the sensitivity of the fluxmeters obtained by calibration [8], outside the phase transition V_0 and V_1 are practically parallel because α changes slightly with temperature. From Fig. 7, we see that the behaviour of V_1 is opposite to that of V_0: the anomaly due to the latent heat appears in V_1 when heating but not when cooling. This behaviour is in agreement with specific heat data c_d and c_r shown in Fig. 3 and it can be explained taking in account that the thermal hysteresis of the sample (about 0.15 K) [22] is higher than the temperature increase produced in the sample during the dissipation branch (about 0.05 K).

Let us consider the measurement process when cooling. The transition temperature is firstly reached at the end or during one of the relaxation periods so that a small fraction of the sample changes of phase. During the following dissipation branch, the temperature of the sample is increased (up to a maximum

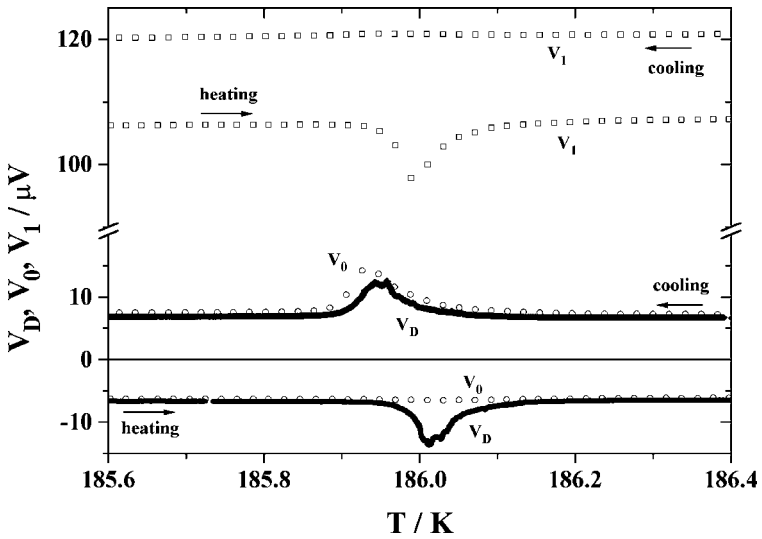

Fig. 7. Measured DTA trace V_D (filled circles), underlying signal V_0 (open circles) and electromotive force at the end of the dissipation branch V_1 (open squares) vs. temperature of the block for $KMnF_3$.

of 0.05 K) but the reversed phase transition is not produced because of the thermal hysteresis of the sample. In conclusion, during the dissipation branch the transition is blocked and there is not effect from the latent heat on V_1 and c_d.

During the following relaxation branch the transition temperature is again reached and a new partial change of phase is produced increasing the molar fraction of the ferroelastic phase. The effect of the latent heat produces the anomaly on V_0 and an increase of the c_r data. During the following dissipation branch the phase transition is blocked again.

In conclusion, the phase transition is produced step by step during the relaxation branch and it is blocked during the dissipation branch, whose effect is to increase the temperature of the sample in a situation where both phases coexist. Thus, the latent heat does not affect c_d and V_1. The phase transition is produced in a temperature range of about 0.2 K which is lower than the theoretical value of the coexistence interval predicted by Landau theory, which was evaluated to be 0.35 K in a previous paper [14].

The same explanation can be used in the heating run. In this case, the behaviour of V_0 and c_d are changed, respectively, by the behaviour of V_1 and c_r.

According to this explanation, specific heat data c_r when heating and c_d when cooling (Fig. 3) represent the right values of $KMnF_3$ specific heat, even inside the coexistence temperature range without any effect from the latent heat. This assumption is supported by the fact that the maximum values of c_r when heating and c_d when cooling agree with the values of c_r when cooling and c_d when heating at the same respective temperatures.

In the case of DKDP sample (Fig. 6), we can see that, despite the small number of V_0 data, the behaviour of V_0 when cooling (positive superposition) is relatively similar to that of V_D trace as it happens in $KMnF_3$ sample. Nevertheless, when heating there is also an anomaly at V_0 although it seems lower than that of V_D trace. This different behaviour can be attributed to the fact the thermal hysteresis in DKDP sample is estimated to be 0.02 K [21], which is lower than the temperature increase during the measurement process (0.05 K), in such a way that the reversed transition is not completely blocked during the opposite superposition.

6. Conclusions

The superposition of a small temperature ramp with long-time periodical square thermal pulses (square modulated thermal analysis) is a very appropriate technique to measure absolute values of specific heat and to study samples near a tricritical point or, in general, when their latent heat is small and specific heat changes significantly around the transition point.

From a first run, we determine absolute values of specific heat. These measurements can be done under electrical field [23], under uniaxial stress [24] or measuring simultaneously other magnitudes such as dielectric susceptibility [25].

Comparing the behaviour of specific heat data obtained in the dissipation or relaxation branch of the square pulse, we can discriminate if a phase transition is discontinuous or not. In the first case, both sets of measurement become different and, in addition, it appears an anomaly in the signal V_0 at the end of each relaxation branch of the pulse.

As we have seen in both samples, the behaviour of V_0 when cooling gives us right idea of the heat flux exchanged by the sample during the phase transition and we can make an approximate evaluation of the latent heat.

If it is necessary a more accurate determination of L, we must carry out a second run with the same temperature ramp but without modulation to obtain the DTA trace. Its comparison with the calculated trace from the specific heat data according to the previously described procedure [6] allow us to determine the value of the latent heat.

With reference to specific heat data in the phase transition interval we must consider two cases:

(a) When latent heat is great enough to produce strong changes of baselines V_0 and V_1, specific heat data are affected by a very significant error and we cannot deduce any consequence.
(b) When latent heat is small enough, the anomaly of the baseline is also small, so that during each measurement, the baseline behaves almost linearly and the errors in the specific heat data are relatively small, showing a regular behaviour. In the case that the increase of temperature of the sample during the dissipation branch be lower than the thermal hysteresis of the sample, it seems that

specific heat data obtained during opposite superposition of modulation and ramp are not affected by the latent heat.

Acknowledgements

We are grateful to A. Gibaud and M. Koralewski for supplying the samples. This work was supported by Project PB98-0115 of the Spanish DGICYT.

References

[1] M. Reading, D. Elliot, V.L. Hill, J. Thermal. Anal. 40 (1993) 949.
[2] I. Hatta, H. Ichikawa, M. Todoki, Thermochim. Acta 267 (1995) 83.
[3] I. Hatta, S. Nakayama, Thermochim. Acta 318 (1998) 21.
[4] J. del Cerro, J. Phys. E Sci. Instrum. 20 (1989) 609.
[5] J. del Cerro, S. Ramos, M. Sanchez-Laulhe, J. Phys. E Sci. Instrum. 20 (1987) 612.
[6] J. del Cerro, F.J. Romero, M.C. Gallardo, S.A. Hayward, J. Jiménez, Thermochim. Acta 343 (2000) 89.
[7] F.J. Romero, M.C. Gallardo, J. Jiménez, J. del Cerro, Thermochim. Acta 372 (2001) 25.
[8] M.C. Gallardo, J. Jiménez, J. del Cerro, Rev. Sci. Instrum. 66 (1995) 5288.
[9] J. Jiménez, E. Rojas, M. Zamora, J. Appl. Phys. 56 (1984) 3353.
[10] V.J. Minkiewicz, Y. Fujii, Y. Yamada, J. Phys. Soc. Jpn. 28 (1970) 443.
[11] R.A. Cowley, Adv. Phys. 29 (1980) 1.
[12] S. Stokka, K. Fossheim, V. Samulionis, Phys. Rev. Lett. 47 (1981) 1740.
[13] S. Stokka, K. Fossheim, J. Phys. C Solid State Phys. 20 (1987) 3417.
[14] S.A. Hayward, F.J. Romero, M.C. Gallardo, J. del Cerro, A. Gibaud, E.K.H. Salje, J. Phys. Cond. Matter 12 (2000) 1133.
[15] U.J. Cox, A. Gibaud, R.A. Cowley, Phys. Rev. Lett. 61 (1988) 982.
[16] A. Gibaud, R.A. Cowley, J. Nouet, Phase Transitions 14 (1989) 129.
[17] A. Gibaud, S.M. Shapiro, J. Nouet, H. You, Phys. Rev. B 44 (1991) 2437.
[18] M.C. Gallardo, F.J. Romero, S.A. Hayward, E.K.H. Salje, J. del Cerro, Mineralogical Magazine 64 (2000) 971.
[19] Landott-Bornstein, Ferroelectrics and Related Substances: Non-oxides, New Series, vols. 16b, 28b, Group III, Springer, Berlin, 1982, 1990.
[20] B. Brezina, A. Fouskova, F. Smutny, Phys. Status Solidii 11 (1972) K149.
[21] M.C. Gallardo, J. Jiménez, M. Koralewski, J. del Cerro, J. Appl. Phys. 81 (6) (1997) 258–2589.
[22] F.J. Romero, M.C. Gallardo, J. Jiménez, J. del Cerro, E.K.H. Salje, J. Phys. Cond. Matter 12 (2000) 4567.
[23] J. del Cerro, J. Thermal Anal. 34 (1988) 335.
[24] M.C. Gallardo, J. Jiménez, J. del Cerro, E.K.H. Salje, J. Phys. Cond. Matter 8 (1996) 83.
[25] J.M. Martín-Olalla, J. del Cerro, S. Ramos, Phase Transitions 64 (1997) 45.